RAA 2014 Vol. **14** No. **7**, 831–842 doi: 10.1088/1674–4527/14/7/005
http://www.raa-journal.org *http://www.iop.org/journals/raa*

Research in Astronomy and Astrophysics

The importance of source positions during radio fine structure observations *

Guennadi P. Chernov[1,2], Yi-Hua Yan[1] and Qi-Jun Fu[1]

[1] Key Laboratory of Solar Activity, National Astronomical Observatory, Chinese Academy of Sciences, Beijing 100012, China; *gchernov@izmiran.ru*

[2] Pushkov Institute of Terrestrial Magnetism, Ionosphere and Radio Wave Propagation, Russian Academy of Sciences (IZMIRAN), Troitsk, Moscow region, 142190, Russia

Received 2013 December 27; accepted 2014 February 28

Abstract The measurement of positions and sizes of radio sources in the observations of the fine structure of solar radio bursts is a determining factor for the selection of the radio emission mechanism. The identical parameters describing the radio sources for zebra structures (ZSs) and fiber bursts confirm there is a common mechanism for both structures. It is very important to measure the size of the source in the corona to determine if it is distributed along the height or if it is point-like. In both models of ZSs (the double plasma resonance (DPR) and the whistler model) the source must be distributed along the height, but by contrast to the stationary source in the DPR model, in the whistler model the source should be moving. Moreover, the direction of the space drift of the radio source must correlate with the frequency drift of stripes in the dynamic spectrum. Some models of ZSs require a local source, for example, the models based on the Bernstein modes, or on explosive instability. The selection of the radio emission mechanism for fast broadband pulsations with millisecond duration also depends on the parameters of their radio sources.

Key words: solar flare — radio emission — zebra-pattern — spike-bursts

1 INTRODUCTION

Zebra-patterns (ZPs), in the form of regular stripes in emission and absorption on the dynamic spectra of solar radiobursts, had already been studied in the fifth solar cycle. Basic observational properties had already been presented in a number of reviews and monographs (Slottje 1981; Kuijpers 1975; Chernov 2006, 2011). Simultaneously, theoretical models were being developed, and at present more than ten mechanisms are being considered. Most often discussed in the literature is the mechanism based on a double plasma resonance (DPR) (Kuijpers 1975; Zheleznyakov & Zlotnik 1975a,b; Kuijpers 1980; Mollwo 1983, 1988; Winglee & Dulk 1986) which assumes that the upper hybrid frequency ($\omega_{\rm UH}$) in the solar corona becomes a multiple of the electron-cyclotron frequency

$$\omega_{\rm UH} = (\omega_{\rm Pe}^2 + \omega_{\rm Be}^2)^{1/2} = s\omega_{\rm Be}, \quad (1)$$

where $\omega_{\rm UH}$ is the upper hybrid frequency, $\omega_{\rm Pe}$ is the electron plasma frequency, $\omega_{\rm Be}$ is the electron cyclotron frequency and s is the integer denoting the harmonic number.

* Supported by the National Natural Science Foundation of China.

This mechanism presents a number of difficulties with the explanation of the dynamics of zebra stripes and some thin effects (sharp changes of frequency drift, a large number of stripes, frequency splitting of stripes and superfine millisecond structure); therefore work on improving this model began to appear (Karlický et al. 2001; LaBelle 2003; Kuznetsov & Tsap 2007). The theory is based on the emission of auroral choruses (magnetospheric bursts) via the escape of the Z mode captured by regular inhomogeneities in plasma density. Kuznetsov & Tsap (2007) assumed that the velocity distribution function of hot electrons within the loss cone can be described by a power law with an exponent of 8–10. In this case, a fairly deep modulation can be achieved.

An alternative mechanism for the ZP was proposed by Chernov (1976, 1990): the coalescence of plasma waves (l) with whistlers (w), such that $l + w \rightarrow t$ (Kuijpers 1975), representing a unified model in which the formation of ZPs was attributed to the oblique propagation of whistlers, while the formation of stripes with a stable negative frequency drift (the fiber bursts) was explained by ducted propagation of waves along a magnetic trap. This model explains the occasionally observed transformation of the ZP stripes into fibers and vice versa.

However, new models are still being proposed. In several works the formation of ZP stripes is explained by radio wave diffraction through heterogeneities in the corona (Laptukhov & Chernov 2006; Bárta & Karlický 2006), or by interference from the straight and reflected (from the heterogeneities) rays (Ledenev et al. 2006). In these cases, the number of harmonics does not depend on the ratio of the plasma frequency to the gyrofrequency in the source. The formation of ZP stripes due to radio wave propagation through heterogeneities in the corona can be recognized as the most natural mechanism of a ZP. However, in this case, only the possibility of generating harmonics in a one-dimensional stationary problem is considered, i.e. the frequency dynamics of stripes are not analyzed.

It is important to note that the whistler model successfully explains the zigzags of stripes and their splitting, and also the synchronous variations in the frequency drift of stripes with the spatial drift of the sources of radio emission (Chernov 2006). Each new phenomenon provides unique parameters describing fine structure, and the entire variety of the parameters does not show a systematic statistical trend (e.g. see Tan et al. 2014). Below, primary attention is given to the analysis of separate phenomena. Such a situation stimulates many authors to elaborate on new mechanisms.

Only positional observations could help to find out where the ZP stripes form (during the excitation of waves in the source or in the course of their further propagation). During the last few years, some new varieties of ZPs have been recorded. In the present paper, an attempt is made to estimate when the positional observations can be the determining factor for the selection of the radio emission mechanism.

In Section 2 several new events are described. Section 3 contains discussion in light of positional observation.

2 LATEST OBSERVATIONS

2.1 2011 February 24 Event

This radioburst had a short duration ($\sim$ 8 min), and in the first 7 min it displayed a smooth type of growth and decay with a number of irregular pulsations in the range 2.6–3.8 GHz. A rich fine structure appeared in the second, more powerful maximum approximately 30 s after 07:37 UT (Fig. 1). The position of the corresponding flare on the eastern limb piques special interest in this event. The flare with importance M3.3 occurred in the active region NOAA 11163 at coordinates N14 E87. This position for the flare made it possible to see two ejections advance into the corona with an interval of $\sim$ 7 min, which were observed in the extreme ultraviolet lines onboard the *Solar Dynamics Observatory* (*SDO*)/AIA, and of the subsequent coronal mass ejection (CME), which was observed in white light by the coronograph *SOHO*/LASCO C2.

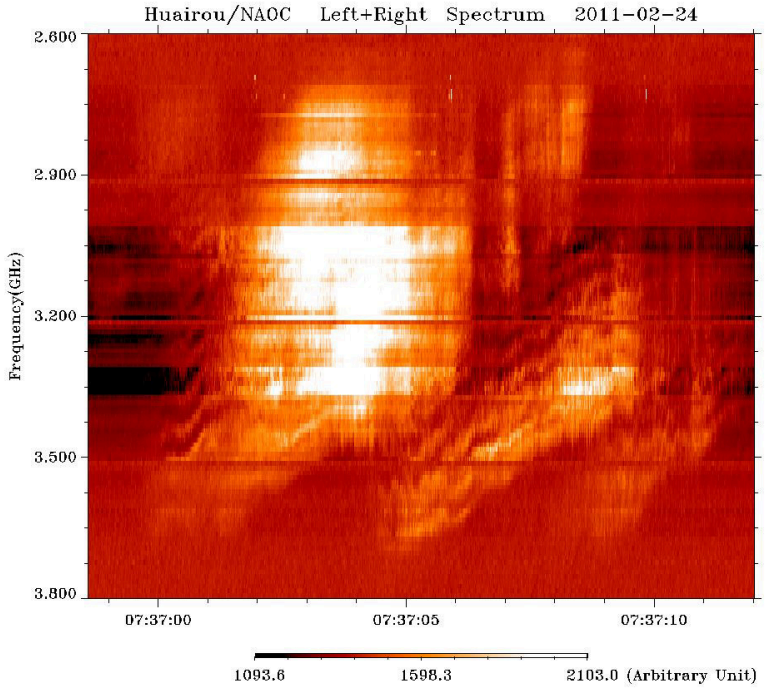

Fig. 1 ZS and pulsation during 13 s registered by the SBRS/Huairou after the second flare ejection on 2011 February 24. The numerous stripes of ZS reveal the superfine structure in the form of millisecond spikes. Radio emission is not polarized.

There were no other flares at this time on the solar disk. The active region 11 161 on the western limb caused a weak flare after only 12 h. Unfortunately, our flare is absent in the flare list of the Nobeyama radioheliograph (RH) (observations ended at 06:20 UT).

In Figure 1 it can be seen that the burst consists of stripes of zebra structure (ZS) which are wavy and drifting with an average speed of $df/dt \sim -60$ MHz s^{-1}. On the low frequency edge of the range, the ZS is washed away, and then pulsations with an irregular period are apparent. The frequency separation between the stripes of ZS decreases with the decrease of frequency from 75 MHz at 3600 MHz to $\sim$ 40 MHz at 3000 MHz. On the high frequency edge of the range, all the emission consists of spikes with a duration of $\sim$ 30 ms. These are usual parameters of ZS in the microwave range, according to Chernov (2011).

Figure 2 presents two frames from the movie made by *SDO*/AIA at 175 Å for the moments of the second ejection coinciding with the second maximum of radio burst where the fine structure in the microwave range is shown in Figure 1.

The beginning of the second ejection at 07:37:02 UT also has the form of a twisted magnetic rope. The frame at the end of this ejection at 07:38:48 UT is the most interesting. It is evident that the magnetic rope extended and went high in the corona. However, its lower part remained at approximately the same height above the point brightening, similar to the X-point of magnetic reconnection, and bright lower loops slightly disperse with the approach to a flare region. The height of this X-point is about 45 000 km; therefore it is possible to consider that the microwave emission of a fine structure must escape from lower altitudes, from the divergent bases of loops. By comparing

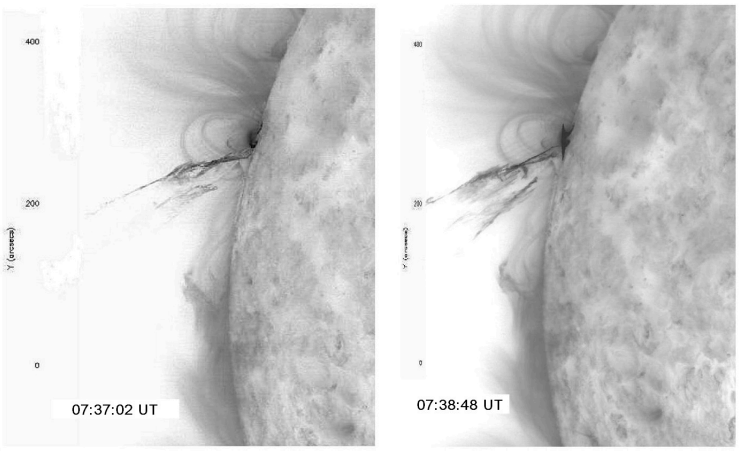

Fig. 2 Two frames from the movie of *SDO*/AIA 171 Å showing the beginning of the second ejection at 07:37:02 UT (*left*) and its continuation at 07:38:48 UT (*right*). In the right frame, the ejection has the form of a magnetic reconnection with an X-point. The thickness of the base of the loop under the X-point is $\leq 1''$.

the two frames in Figure 2 we find the velocity of ejection to be $\sim$ 200 km s^{-1}. If we define the velocity of an agent related with frequency drift of zebra stripes in Figure 1 ($df/dt \sim -60$ MHz s^{-1}) we receive (for instance with the barometric formula) a much higher value, $\sim$ 2000 km s^{-1}, which could be closely correlated with the group velocity of whistler waves.

Thus, we observe for the first time a radioburst from the source with a fine structure in the microwave range at the bases of loops under the X-point of magnetic reconnection. The bases of these loops have a very thin cross section, less than $1''$. The small cross section of this event demonstrates that we need space observations for radio sources.

2.2 Other Events

In Figure 3 the developed ZP with super fine structure is limited from emitting in high frequencies by several fiber bursts. Here is a crucial moment that determines what happens with radio sources when we pass at a fixed frequency from ZP to fiber bursts.

A similar structure was observed previously in the decimeter range (1.1–1.34 GHz) in the 2004 December 1 event shown in Figure 4. With the aid of the position observations it will be possible to verify whether the source of fibers is located below, in the closed loop, and the source of the ZP is located above, in a magnetic island, possibly after a CME occurs. Actually, in the 2010 August 1 event the start of the CME was observed at 07:48 UT, just before the ZS at 08:16 UT (see Liu et al. 2012).

Figure 5 clearly demonstrates another fact: zebra lines also limit the emission of fast pulsations from high frequencies in the event that happened on 2013 April 11.

In such a case, it is only possible to propose that the radio source should be related to magnetic islands after the CME ejection. The particles, accelerated upward in the course of magnetic reconnection, (in the vertical current sheet) only caused pulsations at frequencies lower than 2900 MHz. The particles, accelerated downward, were captured in the magnetic trap, and they are responsible for the formation of zebra stripes. Only with the aid of observations of positions would it be possible to verify such a proposal.

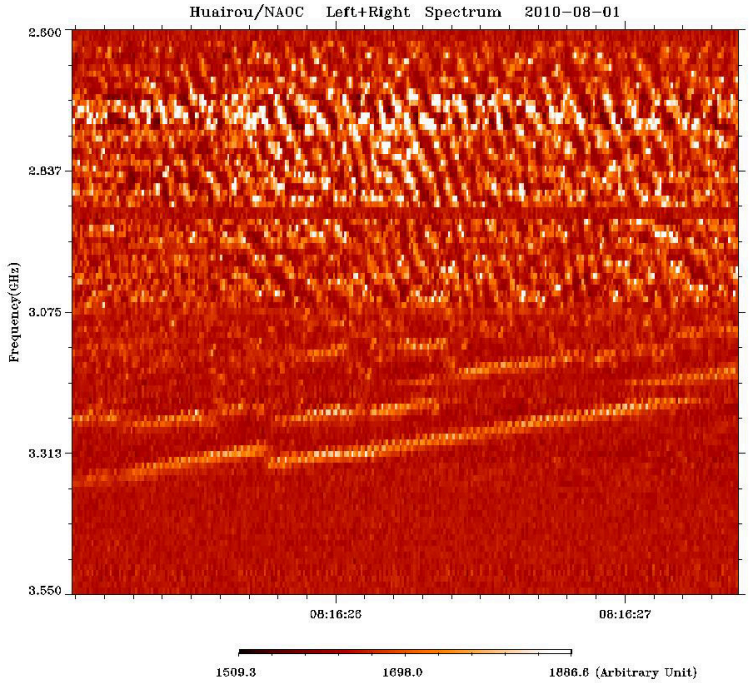

Fig. 3 Fiber burst as a high frequency boundary of a ZP in the 2010 August 1 event.

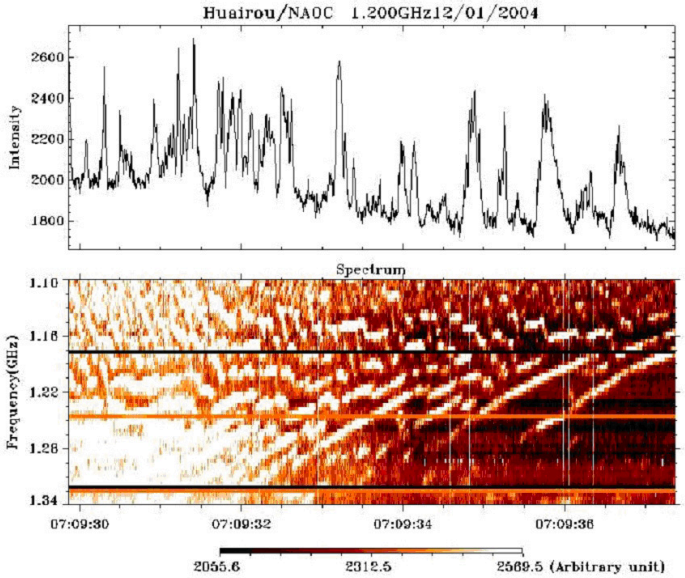

Fig. 4 Fiber burst as a high frequency boundary of a ZP in the 2004 December 1 event in the frequency band 1.2–1.34 GHz. The intensity profile at 1.2 GHz in the top panel shows superfine structure in the ZS which is not very evident in fiber bursts.

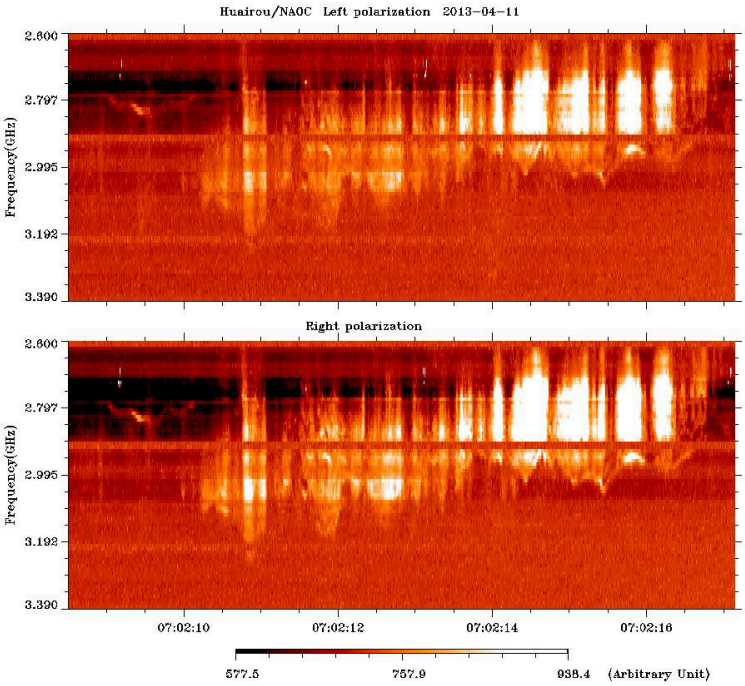

Fig. 5 Fast pulsations that lasted 8 s and were registered by the SBRS/Huairou in the event on 2013 April 11. The emission is limited from emitting in high frequencies by several zebra stripes.

3 DISCUSSION

3.1 Choice of ZP Model Using Positional Observation

The measurement of positions and sizes of radio sources in the observations of the fine structure of solar radio bursts is the determining factor for the selection of the radio emission mechanism. The identical parameters of the radio sources for ZSs and fiber bursts confirm that there is a common mechanism for both structures.

The newly-examined events show that the ZSs and fiber bursts can appear almost simultaneously or consecutively in the microwave, decimeter and meter wavebands.

The most cited and used model to describe ZPs is the mechanism of DPR, especially after the paper of Chen et al. (2011) where the authors allegedly confirm this mechanism using positional observations by the Frequency-Agile Solar Radiotelescope (FASR) Subsystem Testbed (FST). In this line of research, it is necessary to note that the whistler model was mistakenly rejected. In the whistler model, when we estimate $V_{\rm gr} = 2.5 \times 10^9$ cm s^{-1}, it is the value in the quasi-longitudinal propagation (along the magnetic trap, it is not $V_{\rm proj}$ as authors used). $V_{\rm proj} = V_{\rm gr} \times \cos\alpha 1$, then for wide angle propagation of a whistler ($\cos\alpha 1 \sim 0.1$) the same value of $\tan\alpha 1$ as for $\tan\alpha 2$ is obtained (see Fig. 6). So, there is no problem with the whistler model. The high speed of spatial drift for the zebra sources ($\sim 0.1c$) can be related to a higher density gradient across the magnetic trap. Then, Chen et al. (2011) used convenient idealistic models for plasma density and magnetic field with exponential dependence, instead of the well-known barometric formula and dipole dependence for B (or model of Dulk & McLean 1978).

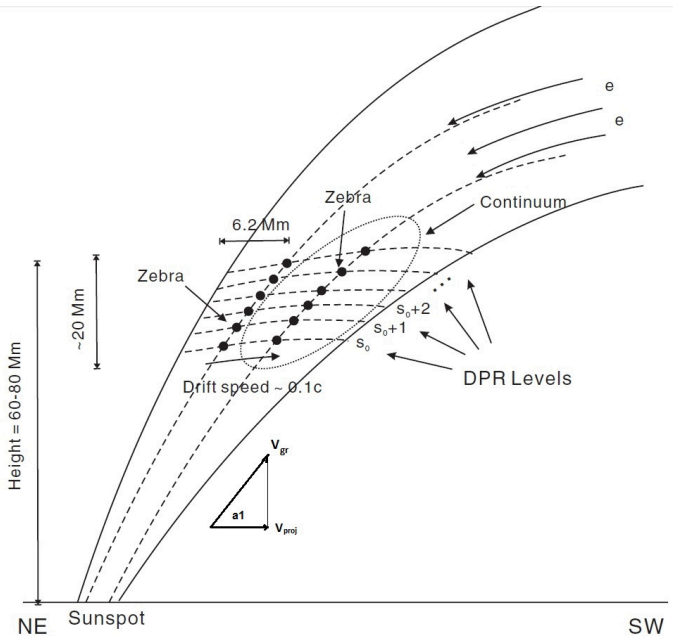

Fig. 6 Simplified source model (fig. 14 from Chen et al. 2011), supplemented by the vector representing the group velocity.

In the decimeter range an attempt at determining the displacement of the source during one of the zebra stripes in the phenomenon on 2006 December 14 with the aid of the FASR system did not succeed because of insufficient time resolution, ~ 20 ms approximately in the same time interval.

The location of the ZP emission centroid was defined by the intersection of the three interferometric fringes of FST. The interferometric phase conveys the spatial information of the radiation source. Unfortunately, Chen et al. (2011) considered averages of the phases "along" the on- and off-stripe positions (in time), to reveal the spatial distribution of the source of the ZP over frequency. The height of the source was determined by an indirect method: by the extrapolation of the magnetic field above the active region in combination with an arbitrarily selected density model.

In the phenomena on the limb (like the 2011 February 24 event, Fig. 2), position observations allow the determination of the real height of the radio source above the photosphere and by that to choose the real model of density. Estimations of the magnetic field strength according to the frequency separation between zebra stripes could be bound by the specific height in the corona. Such data regarding density and magnetic field strength at the specific height are decisive factors for the selection of the generation mechanism. For the phenomena on the disk, the value of the projection of the height of the source on the picture plane should be divided by the sine of longitude (for a rough estimate).

3.2 Several New ZP Models

Similar discussions stimulate the developments of new models. Treumann et al. (2011) proposed a new mechanism to generate a ZP, the ion-cyclotron maser. Thanks to the special delta-shaped distribution function of the accelerated ions, the ion-cyclotron maser generates a number of electromag-

netic ion-cyclotron harmonics which modulate the electron maser emission. Some of the accelerated relativistic protons pass along the magnetic field across the trapped loss-cone electron distribution. The modulation of the loss-cone will necessarily cause a modulation of the electron cyclotron maser. Locally, this produces the typical "zebra" emission/absorption bands. However this mechanism can work in a strong magnetic field, when $f_{\rm pe}/f_{\rm ce} < 1$.

Karlický et al. (2013) continued the development of the model of Kuznetsov (2006) for fiber bursts: fiber bursts can be explained by the propagating fast sausage magnetoacoustic wave train. Then Karlický (2013) extended a similar model for ZP: the magneto-acoustic waves with density variations that modulate the radio continua, and this modulation generates zebra effects. It should be noted that a close model based on propagation through inhomogeneities was examined in more detail by Laptukhov & Chernov (2009, 2012).

Yurovsky (2011) continued a series of works about the formation of a ZP due to the refraction (interference mechanism) of rays in the heterogeneities in the corona. However, the author does not refer to the previous works (Ledenev et al. 2006), and carried out a simplified simulation of ZP stripes which coincides with those observed cases.

3.3 The Form of Radio Source

It is easy to divide all known models into two classes in terms of their radiation source: distributed by height or local (a quasi-point source).

In both models of ZS (the DPR and the whistler) the source must be distributed along the height, but in contrast to the stationary source in the DPR model, in the whistler model the source should be moving. Moreover, the direction of the space drift for the radio source must correlate with the frequency drift of stripes in the dynamic spectrum. Such a correlation is known in the meter range with one-dimensional source positions of Nançay RH at 236.6 MHz (see fig. 16 in Chernov 2006).

In the interference models (Ledenev et al. 2006; Yurovsky 2011) two sources must be visible (the direct ray and the reflected one). Some models of ZS require a local source, for example, models based on the Bernstein modes, and probably in the new model with ion cyclotron harmonics by Treumann et al. (2011), or based on explosive instability (Fomichev et al. 2009). The selection of the radio emission mechanism for fast broadband pulsations with millisecond duration also depends on the parameters of their radio sources.

3.4 Several Crucial Phenomena

Figure 7 shows fiber bursts immerged into a ZP in the 2004 December 1 event. It is very important to know whether both elements have the same radio source but different emission mechanisms.

In several events, drifting bands (similar to a type-II burst in the meter range) were observed (Fig. 8). It is very important to know whether the radio source is moving (in the form of a shock wave) or not. For the 2004 September 12 event we have an observation of the position with the Nobeyama RH at 17 GHz, and actually, just at the moment 00:35:46 UT (shown in Fig. 8) we see an ejection above the leading spot of the active region into the southern direction. However, the positions of the sources at 17 and 3 GHz can be different, but possibly, the ejection continues higher into the corona.

Later in the same event zebra stripes with wavy frequency drifts were observed. Figure 9 presents an excellent example to verify synchronous changing of spatial drift of the radio source in the whistler model.

In many previously observed events, we cannot understand the nature of the radio source without positional observations. A good example is shown in Figure 10.

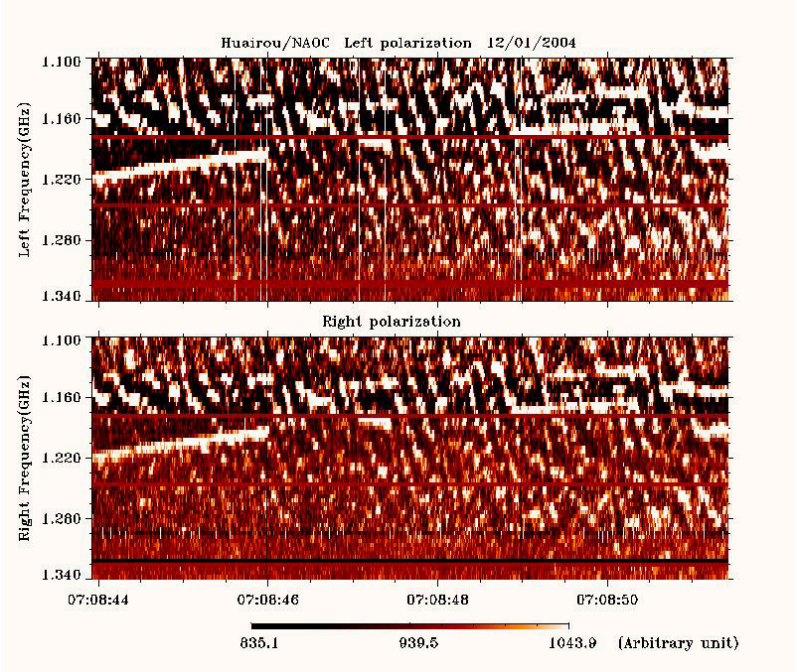

Fig. 7 The 2004 December 1 event. Fiber bursts are immerged into the ZP. Zebra stripes consist of spikes, however fiber bursts are almost continuous (uninterrupted).

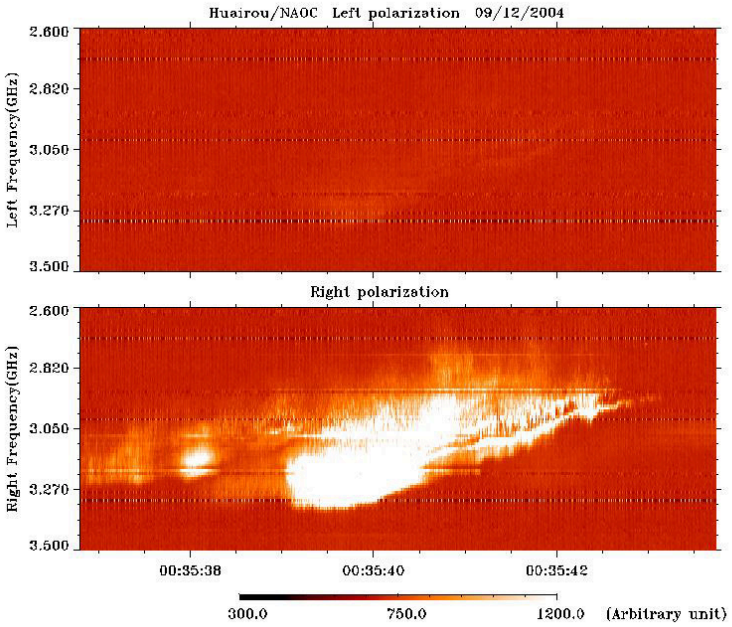

Fig. 8 Unusual burst in the range 2.7–3.4 GHz in the event that occurred on 2004 September 12. This burst is similar to meter type II bursts.

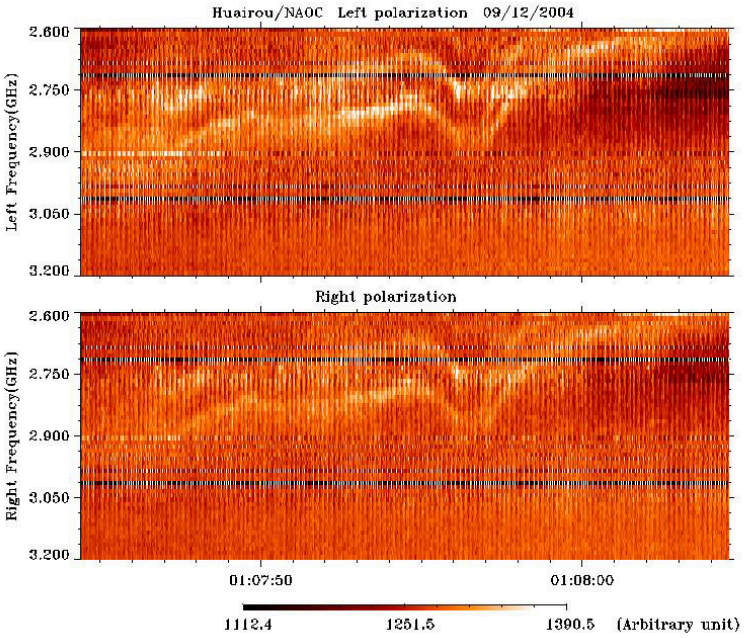

Fig. 9 What happens with a radio source during such oscillation and bifurcation of zebra stripes?

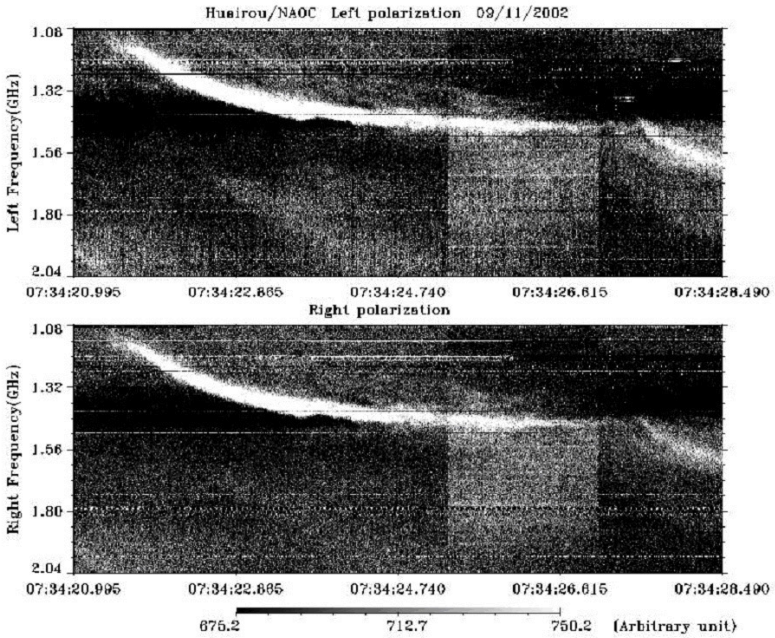

Fig. 10 A strange burst in the range 1–1.5 GHz in the event that occurred on 2002 September 11. The narrow stripe (of $\sim$ 50 MHz) has decreasing frequency drift which could be caused by the deceleration of an exciter in the corona.

3.5 Possibility of One Dimensional Positional Observations and New Instruments

Regarding ZPs, we can understand much even from one-dimensional observations, which are shown in figure 8 in Chernov et al. (2013). They depict the group of spikes recorded by the Siberian Solar Radio Telescope (SSRT) at 5.7 GHz and a spectrum obtained at Purple Mountain Observatory (PMO). However, each source in the SSRT map combines several spikes as it is visible at the top panel with the PMO spectrum and intensity profile of SSRT. This is due to the insufficient time resolution of SSRT (15 ms) in comparison with the resolution in the PMO spectrum (5 ms). Nonetheless, we see there small shifts in centers of spike sources. Moreover, Chernov et al. (2013) have shown how simultaneous one-dimensional observations in E-W and N-S directions allow locating the sources of spikes on a two-dimensional map. The sources were scattered along an arcade of flare loops. In the zebra source we expect systematic movement along zebra stripes.

Now, we hope for progress in the field of solar radio spectral imaging observations. The Chinese spectral radioheliograph (CSRH) is a new generation solar radio telescope which will be the largest and most advanced radio imaging telescope for imaging the solar corona in the world. It can provide true imaging spectroscopy with high temporal, spatial and spectral resolutions, covering decimeter and centimeter wavelengths.

In the decimeter range (0.4–2 GHz) 40 antennas, each with a diameter of 4.5 m, in CSRH I will provide spatial resolution of $10.3''$ at 2 GHz, and CSRH II, having 60 antennas each with a diameter of 2 m, will provide spatial resolution of $1.4''$ at 15 GHz (Yan et al. 2009; Yan et al. 2013).

We also await new possibilities from the upgraded SSRT; a radioheliograph with 96 antennas in the range 4–8 GHz, which will each construct one image at one frequency 0.1–1 s (Lesovoi et al. 2014).

4 CONCLUSIONS

We demonstrated several events with radio fine structures in which the positional observations could be a determining factor for the selection of the radio emission mechanism.

It is very important to compare the source sizes of continuum and different fine structures, and to know whether the radio source is moving (in the form of a shock wave) or not.

Radio sources of fiber bursts and ZPs in the whistler model must have moving sources, and the spatial drift of ZP stripes should change synchronously with changes of frequency drift in the dynamical spectrum. In the DPR model the ZP source must be rather stationary.

Acknowledgements The authors are grateful to the Nobeyama, *TRACE*, *RHESSI*, *SOHO* (LASCO/EIT) and *SDO* teams for operating the instruments and performing the basic data reduction, and especially for the open data policy. The research carried out by G.P. Chernov at National Astronomical Observatories, Chinese Academy of Sciences (NAOC) was supported by the Chinese Academy of Sciences Visiting Professorship for Senior International Scientists, grant No. 2011T1J20. The work was partially supported by the Russian Foundation of Basic Research (RFBR), grant No. 14-02-00367. The National Basic Research Program of China (973 program, Grant No. 2006CB806301) and CAS-NSFC Key Project (Grant No. 10778605) have supported the Chinese authors.

References

Bárta, M., & Karlický, M. 2006, A&A, 450, 359
Chen, B., Bastian, T. S., Gary, D. E., & Jing, J. 2011, ApJ, 736, 64
Chernov, G. P. 1976, Soviet Ast., 20, 582
Chernov, G. P. 1990, Sol. Phys., 130, 75
Chernov, G. P. 2006, Space Sci. Rev., 127, 195

Chernov, G. 2011, Fine Structure of Solar Radio Bursts (Berlin: Springer)
Chernov, G. P., Sych, R. A., Huang, G.-L., et al. 2013, RAA (Research in Astronomy and Astrophysics), 13, 115
Dulk, G. A., & McLean, D. J. 1978, Sol. Phys., 57, 279
Fomichev, V. V., Fainshtein, S. M., & Chernov, G. P. 2009, Plasma Physics Reports, 35, 1032
Karlický, M. 2013, A&A, 552, A90
Karlický, M., Bárta, M., Jiřička, K., et al. 2001, A&A, 375, 638
Karlický, M., Mészárosová, H., & Jelínek, P. 2013, A&A, 550, A1
Kuijpers, J. 1980, in Radio Physics of the Sun, IAU Symposium, 86, eds. M. R. Kundu & T. E. Gergely, 341
Kuijpers, J. M. E. 1975, Collective Wave-particle Interactions in Solar Type IV Radio Sources, Ph.D. thesis, Utrecht University
Kuznetsov, A. A. 2006, Sol. Phys., 237, 153
Kuznetsov, A. A., & Tsap, Y. T. 2007, Sol. Phys., 241, 127
LaBelle J., Treumann R. A., Yoon P. H., Karlicky M., 2003, Astrophys. J., 593, 1195
Laptukhov, A. I., & Chernov, G. P. 2006, Plasma Physics Reports, 32, 866
Laptukhov, A. I., & Chernov, G. P. 2009, Plasma Physics Reports, 35, 160
Laptukhov, A. I., & Chernov, G. P. 2012, Plasma Physics Reports, 38, 560
Ledenev, V. G., Yan, Y., & Fu, Q. 2006, Sol. Phys., 233, 129
Lesovoi, S. V., Altyntsev, A. T., Ivanov, E. F., & Gubin, A. V. 2014, RAA (Research in Astronomy and Astrophysics), 14, 864
Liu, Y. D., Luhmann, J. G., Möstl, C., et al. 2012, ApJ, 746, L15
Mollwo, L. 1983, Sol. Phys., 83, 305
Mollwo, L. 1988, Sol. Phys., 116, 323
Slottje, C., 1981, Atlas of fine Structures of Dynamic Spectra of Solar Type IV-dm and Some Type II Bursts, Utrecht Observatory, 2
Tan, B., Tan, C., Zhang, Y., Mészárosová, H., & Karlický, M. 2014, ApJ, 780, 129
Treumann, R. A., Nakamura, R., & Baumjohann, W. 2011, Annales Geophysicae, 29, 1673
Winglee, R. M., & Dulk, G. A. 1986, ApJ, 307, 808
Yan, Y., Zhang, J., Wang, W., et al. 2009, Earth Moon and Planets, 104, 97
Yan, Y., Wang, W., Liu, F., et al. 2013, in IAU Symposium, 294, eds. A. G. Kosovichev, E. de Gouveia Dal Pino, & Y. Yan, 489
Yurovsky, Y. F. 2011, Bulletin Crimean Astrophysical Observatory, 107, 84
Zheleznyakov, V. V., & Zlotnik, E. I. 1975a, Sol. Phys., 44, 447
Zheleznyakov, V. V., & Zlotnik, E. Y. 1975b, Sol. Phys., 44, 461